PAPER No. 69

FRACTURE MECHANICS OF MATRIX CRACKING AND DELAMINATION IN GLASS/EPOXY LAMINATES

M. Caslini and C. Zanotti
Laboratorio Tecnologie Sperimentali
Costruzioni Aeronautiche G. AGUSTA
21013 Gallarate, ITALY

and

T. K. O'Brien
U.S. Army Aerostructures Directorate
U.S. Army Aviation Research and Technology Activity (AVSCOM)
NASA Langley Research Center
Hampton, Virginia 23665-5225
U.S.A.

ABSTRACT

This study focused on characterizing matrix cracking and delamination behavior in multidirectional laminates. Static tension and tension-tension fatigue tests were conducted on two different layups. Damage onset, accumulation, and residual properties were measured. Matrix cracking was shown to have a considerable influence on residual stiffness of glass epoxy laminates, and could be predicted reasonably well for cracks in 90° plies using a simple shear lag analysis. A fracture mechanics analysis for the strain energy release rate associated with 90° ply matrix crack formation was developed and was shown to correlate the onset of 90° ply cracks in different laminates. The linear degradation of laminate modulus with delamination area, previously observed for graphite epoxy laminates, was predicted for glass epoxy laminates using a simple rule of mixtures analysis. The strain energy release rate associated with edge delamination formation under static and cyclic loading was difficult to analyze because of the presence of several contemporary damage phenomena.

1. INTRODUCTION

The application of composite materials in modern helicopters is being extended to more complex and safety-critical components which require a deeper understanding of the material behavior to guarantee reliability. In the future, civil and military authorities may require a failsafe or damage-tolerant design of composite helicopters. This need is recognized in principle by the helicopter manufacturers, but it is clear that material properties, test methods, and application of composites to real components must be further investigated in order to achieve reliable structures. Because glass/epoxy composites are already being used extensively in helicopter rotor systems, an investigation of the fatigue behavior of glass/epoxy laminates was undertaken in the hopes of laying a foundation for future damage assessment of helicopter structural components.

Composite laminates commonly employed in helicopters, as in many other applications, usually show evidence of damage before failure. The usually adopted "first ply failure" criterion [1] can very roughly predict transverse ply matrix cracking but cannot predict delamination. Both of these two damage

modes may occur early in the life of the component but may have only a small effect on overall stiffness and strength properties.

The scope of this work is to study these two phenomena from a fracture mechanics point of view, offering, as far as possible, some simple but reliable criteria to predict onset and accumulation of matrix cracking and delamination. Extensive work has already been done with good results using fracture mechanics to model both delamination [2-5] and matrix cracking [5-13], but only in a few cases are these results readily applicable to design.

In this work a new approach is developed for characterizing matrix cracking onset and growth. The critical strain energy release rate for formation and accumulation of matrix cracking in the 90° plies of $[0/90]_s$ and $[\pm 45/0/90]_s$ glass/epoxy composites were calculated and plotted for a range of crack densities in the transverse plies.

A previously developed closed form model is available to predict edge delamination behavior in composite laminates [2]. In the present study this model was applied to glass/epoxy quasi-isotropic laminates, where the presence of pre-existing matrix cracking was observed. The theoretical model was then compared with experimental results. Critical strain energy release rates associated with edge delamination were measured for the material studied.

2. EXPERIMENTS

Two E glass/epoxy laminates were tested in quasi-static tension and in tension-tension fatigue. The material was T190/X751/50[1] with an average ply thickness of .225 mm, 50% fiber volume, 125 °C curing temperature. The measured tensile failure strain in the fiber direction was 1.76% and the following elastic properties were measured from unidirectional specimens:

$$E_1 = 43.7 \text{ GPa} \qquad E_2 = 16.0 \text{ GPa}$$
$$G_{12} = 6.3 \text{ GPa} \qquad \nu_{12} = .284$$

The layups tested were $[0/90]_s$ and $[\pm 45/0/90]_s$. The first sequence was chosen to isolate the 90° ply matrix cracking from other damage phenomena; the second sequence was chosen to highlight the edge delamination at the 0/90 interface, because of the high peeling stresses which are generated [2]. Tests were run on an Instron servo-hydraulic machine. Axial strain was derived from displacements measured by a pair of LVDT's over an 82 mm gage length. A high intensity light was shone through the specimen to observe and photograph the damage. Matrix crack density and delamination were measured from high contrast photographic prints like the one shown in fig. 1. For each laminate five quasi-static tension tests were run with a ram speed of 0.5 mm/min. At specified loads the specimens were unloaded to record damage and residual stiffness (tangent modulus). Tension-tension load-controlled fatigue tests were conducted with a repeated sinusoidal load of 6 Hz frequency and 0.1 load ratio; 20 fatigue tests for the $[0/90]_s$ lay-up and 25 tests for the $[\pm 45/0/90]_s$ lay-up were performed, covering the whole range of possible fatigue lives from 1 to 10^6 cycles. The cyclic loading was interrupted at specified intervals, to monitor damage and measure static stiffness.

(1) Produced by Cyanamid Fothergill Ltd., U.K.

3.DAMAGE OBSERVATIONS

Figure 2 shows schematically the damage types observed on quasi-isotropic specimens, namely 90° ply matrix cracking, edge delamination at the 0/90 interface and local delaminations originating from the angle ply cracks. Depending on the type of test (static or fatigue) and on the load levels, damage accumulation showed some qualitative and quantitative differences.

From previous works it is known that matrix cracks do not grow indefinitely in number, instead they reach a "saturation value", which seems to be a function of the laminate characteristics [8]. In static tests failure occurred when the number of 90° ply matrix cracks was still low and angle-ply cracks had not yet developed. The edge delamination at failure was extended over 20% of the interfacial area and the stiffness loss was typically about 15% of the initial stiffness.

Fatigue damage accumulation is shown in fig.3. This figure shows the results of a single test run at 160 MPa maximum sinusoidal load (R=0.1), which is about 60% of the laminate static failure stress, and is typical for damage developed during fatigue tests, run on quasi isotropic glass epoxy laminates .

The build up of the laminate damage is plotted against fatigue cycles. Figure 3(a) shows the matrix cracking formation in 90°, +45° (external) and -45° (internal) plies. For each of these plies, matrix cracks reach a saturation level at different number of cycles. The cracks in the 90° plies accumulate faster than matrix cracks in the others, so that all other damage may be considered to happen after the 90° plies damage reached saturation. Fig.3(b) displays the edge delamination and local delaminations growth. Comparing fig.3(a) and 3(b), the delaminations and cracking of +45 and -45 plies appear to be almost contemporary, so that their effects must be superimposed. The cumulative effect of the damage on the specimen longitudinal modulus E/E_0 is shown in fig 3(c).

The same type of tests were performed on $[0/90]_s$ laminates in order to isolate the behavior of 90° ply matrix cracking. The $[0/90]_s$ laminate showed only 90° matrix cracking in static tests. Also in fatigue, the damage was mainly 90° matrix cracking, but the onset of matrix cracking in 0° plies, i.e. longitudinal splits, was observed before final failure. Total stiffness loss just before failure was 15% in static tests and more than 20% in fatigue tests.

4.ANALYSIS OF MATRIX CRACKING

Matrix cracking occurs when tensile stresses normal to the fibers are present. On glass reinforced composite materials this kind of damage is responsible for a considerable fraction of the total stiffness loss both in static and in fatigue tests. To predict the matrix cracking effect on different laminates and loadings, available models have been studied and compared to experimental results, and a fracture mechanics approach has been applied to characterize matrix crack onset and growth.

4.1.Stiffness loss in a $[0_m/90_n]_s$ laminate (See Fig.4)

A closed form expression for stiffness loss in a $[0_m/90_n]_s$ laminate as a function of crack density D (fig. 4) was derived previously from a shear lag analysis [13] as

$$\frac{E_x}{E_0} = \frac{1}{1 + \frac{nE_2}{mE_1}\,\frac{\tanh(\lambda/2D)}{\lambda/2D}} \qquad (1)$$

where

$$\lambda^2 = \frac{3}{h^2}\,\frac{G_{12}}{E_1}\,\frac{E_0}{E_2}\,\frac{(n+m)}{n^2 m}$$

and E_x, E_0 are the moduli of the cracked and the uncracked laminate respectively. The E_1, E_2 and G_{12} are the lamina longitudinal, transverse and shear moduli respectively, and h is the ply thickness.

To evaluate the degree of approximation introduced by eq.(1) in the laminates presently studied, this equation has been compared with results from a NASTRAN finite element model [24] and with experimental data. Fig.5 compares equation (1) (continuous line) and F.E.M. results (diamonds and dashed line) with data obtained in static and fatigue tests on $[0/90]_s$ laminates. The small difference observed between the finite element results and eq.(1) will produce consequences that will be discussed later. The comparison with the experimental data also confirmed the validity of equation (1) for elevated crack densities.

4.2.Stiffness Loss in Other Laminates

Although equation (1) is only valid for $[0_m/90_n]$ stacking sequences, its use can be extended to model stiffness loss due to matrix cracking in the 90° plies, surrounded by 0° laminae, in other laminates of arbitrary orientation. Previously, a technique was developed for estimating the reduction in E_2 for a cracked 90° ply as a function of the crack density [6]. This technique is depicted in fig.6. First, the reduction in laminate modulus, E_x/E_0, of a $[0/90]_s$ laminate is determined as a function of the crack density in the 90° ply (fig. 6(a)). In the current study, this was determined using eq.1 (fig.5). Next, the linear relationship between the reduced value of E_2 in the cracked 90° ply and the $[0/90]_s$ laminate modulus is calculated from laminated plate theory (fig. 6(b)). The reduced laminate modulus, E_x/E_0, calculated when the effective transverse lamina modulus in the 90° ply, E_2'/E_2, is set to zero is designated $E_\#/E_0$, and is the value obtained from the ply discount method where the cracked 90° ply is assumed to carry no load. Finally, the equation of the straight line, relating E_2'/E_2 to E_x/E_0 (fig. 6(b)), is combined with the equation describing E_x/E_0 as a function of crack density (fig. 6(a)) to generate the equation for a master curve relating the effective transverse modulus of a cracked 90° ply in an arbitrary laminate, E_2'/E_2, to the crack density in that 90° ply (fig 6(c)). This master curve may then be used to determine the appropriate reduction in E_2 for a cracked 90° ply in another laminate, such as the $[45/-45/0/90]_s$ laminate tested in the current study.

In ref.6 it was assumed that the longitudinal modulus of a laminate with matrix cracks is a linear function of the " effective damaged lamina " transverse modulus E' normalized to the undamaged lamina transverse modulus E_2 (fig. 6(b)). The equation of this straight line yields:

$$\frac{E_2'(D,w)}{E} = \frac{E_x(D,w) - E_\#}{E_0 - E_\#} \qquad (2)$$

In reference 6, the finite element method was used to determine the $[0/90]_s$ laminate stiffness loss as a function of crack density, $E_x(D,w)$, whereas in the present study it was possible to start from a closed form expression (eq.1). Equation (2) may be rearranged to yield

$$E_x = E_\# + (E_0 - E_\#)\,\frac{E'}{E_2} \qquad (3)$$

A precise expression of eq. 3 may be obtained through laminated plate theory [24], but the result shows no significant difference from eq. 3.

Eq. 2 gives E'/E_2 as a function of crack density and ply thickness, w=2nh (fig. 4), for a laminate stacking sequence where the relationship between E_x and D·w is known. In the present case, a $[0/90]_s$ glass/epoxy laminate was modeled using equation (1). This approach is valid only if the 90° ply is constrained by adjacent 0° plies. For other cases, where more complex shear stresses are involved, the relationship between E_x and crack density may be obtained from finite element analysis and substituted into eq.2 to determine the functional relationship between E'_2/E_2 and crack density.

To check the validity of representing the effect of transverse ply cracking on laminate stiffness in terms of a calculated effective modulus $E'_2(D,w)$, the longitudinal modulus of a $[\pm 45/0/90]_s$ laminate was calculated and plotted in fig.7 (solid line) for several 90^0 ply crack densities using $E'_2(D,w)$ for the cracked 90° plies obtained from eq.2. The quasi-isotropic laminate containing various crack densities was also modeled using the NASTRAN finite element code [24]. The laminate stiffnesses calculated by FEM are shown in fig.7 as diamond symbols connected by a dashed line. The agreement between the calculated stiffness loss, from eq.2 and FEM, and the experimental data (triangles in fig. 7) was fairly good.

4.3. Strain Energy Release Rate

A fracture mechanics analysis was applied to develop a tool capable of predicting onset and growth of matrix cracking. For an elastic body containing a flaw of area A that extends under a constant nominal strain, ε, the strain energy release rate, G, may be written as

$$G = -V \frac{\varepsilon^2}{2} \frac{dE}{dA} \qquad (4)$$

where V is the volume of the body and dE/dA is the rate of stiffness change as the flaw extends [2].

The fundamental assumption of this work is that all of the N matrix cracks in the volume V may be treated as a single equivalent flaw of area A, that is

$$A = \sum_{i=1}^{N} A_i \qquad (5)$$

and that all the matrix cracks have the same length, w, equal to the thickness of the cracked laminae (fig. 4). Therefore, for a laminate of width, 2b, length, ℓ, and total thickness, t,

$$A = N\ 2b\ w, \text{ and } V = 2b\ \ell\ t \qquad (6)$$

Because $N = \ell\ D$, A can be espressed in terms of crack density D:

$$A = 2b\ \ell\ w\ D, \text{ and } dA = 2b\ \ell\ w\ dD$$

With these assumptions G may be written as

$$G = -\frac{t}{w} \frac{\varepsilon^2}{2} \frac{dE}{dD} \qquad (7)$$

Differentiating eq. 1 and substituting into eq. 7 yields a closed form expression of the strain energy release rate for matrix cracking in a $[0_m/90_n]_s$ laminate:

$$G = \frac{(n+m)}{m} \frac{E_2}{E_1} \frac{E_0}{D} \frac{\varepsilon^2}{2} \left[\frac{\frac{\tanh(\lambda/2D)}{\lambda/2D} - \frac{1}{\cosh^2(\lambda/2D)}}{\left[1 + \frac{nE_2}{mE_1} \frac{\tanh(\lambda/2D)}{\lambda/2D}\right]^2} \right] \qquad (8)$$

The closed form expression is particularly suitable for comparing different lay-ups and materials. Fig.8 shows the calculated effect on strain energy release rates of different lay-ups and reinforcing fibers. In the case of Glass fibers (solid and dashed curves), the effects of doubling either the 90° or the 0° ply thickness are shown. Doubling the 90° ply thickness results in a doubling of the strain energy release rate, as it is evident comparing the curves for the $[0/90]_s$ and $[0/90_2]_s$ laminates. Doubling the number of 0° plies, however, has very little effect on G as seen when comparing the curves for the $[0/90_2]_s$ and $[0_2/90_2]_s$ laminates. The difference in the G curves for these two laminates is greatest at small values of crack density. Hence, the onset of 90° matrix cracks may occur differently for the two laminates, but the accumulation of cracks should be similar for both. Figure 8 also shows a comparison of $(0/90)_s$ glass/epoxy and graphite/epoxy laminates. As expected, graphite/epoxy shows a lower and flatter G curve, because 90° ply matrix cracking has a lesser effect on laminate stiffness in graphite/epoxy compared to glass/epoxy [2].

Figure 9 compares strain energy release rate as a function of crack density, for a $[0/90]_s$ glass/epoxy laminate, calculated both from eq. 8, and from eq. 7 using dE/dD derived from finite element results. The difference in the G values from the two techniques results from the difference in slope of the stiffness vs. crack density expressions, which can be observed in figure 5. At the moment, it is not possible to establish which of the two models is closer to the actual behavior in the initial region of low crack density, since both rely on some simplifying assumptions, and the scatter in the experimental data shown in fig. 5 makes it difficult to resolve which analysis is more appropriate. In the high crack density region, however, the finite element analysis seems to comply better with the experimental data and with the assumption that for high crack density G must reach zero in order to explain the observed phenomenon of crack density saturation.

4.4.Matrix crack onset

To evaluate G_c for the onset of 90° ply matrix cracking in a $[0_m/90_n]_s$ laminate, it is easier to use a simpler form of eq. 8 with D set to zero

$$G_c = \frac{(n+m)}{m} \frac{E_2}{E_1} \frac{E_a}{\lambda} \varepsilon_c^2 \qquad (9)$$

A similar expression was derived from a shear lag analysis in ref.[10] and [11]. Equation 9 differs only in that the factor 3 included in the λ expression (eq.1) is replaced by a 4 in ref.[10] and [11]. This difference is a result of the different distributions of the longitudinal displacements in the transverse ply used in the shear lag analysis. This distribution was parabolic in the derivation of eq. 1 [13] and linear in ref. 10.

For a generic laminate with 90° plies surrounded by 0° plies, dE/dD is easily calculated from eq.(2) when D=0. This calculation introduces an approximate linearized expression for effective damaged lamina transverse modulus, obtained from eq.(1), as D approaches zero.

4.5.Crack growth

As crack density increases, eq. 8 gives a lower value of G for a fixed strain. In a constant strain fatigue test no more cracks should appear, as soon as G is reduced below its critical value. In the present study, where all the tests were run under load control, an experimental proof was not possible and, as already stated, in most cases the matrix cracks reached a saturation density value. The presence of this saturation density is not totally explained with the

closed form expression, because in eq.8, the dE/dA term never goes to zero. If dE/dA does not go to zero, then an increased stress will always generate more cracks. The finite elements analysis however, shows more clearly that dE/dA is very close to zero when the crack density is near to the saturation value, no matter what the stress level (fig. 9).

Looking at the problem from another point of view, the "apparent" critical G value, G_R, would increase with increasing crack density. Therefore, a crack resistance curve concept was borrowed from classical fracture mechanics [17], showing the progressive laminate resistance to formation of new matrix cracks as the number of these cracks increases. This increased crack growth resistance is not attributed to other energy absorbing damage mechanisms, but results only from the constraint and load transfer capability of the neighboring plies adjacent to the cracked ply.

Crack growth resistance curves (R-curves) for 90° ply matrix cracking were obtained from quasi-static tension tests. Five tests of this kind were performed on $[0/90]_s$ and $[\pm 45/0/90]_s$ laminates. Figure 10 shows G_R calculated from strain and crack density data for both laminates, using equation (8). The first point plotted for each curve corresponds to the onset of the first matrix crack, and shows G_c as would be calculated from eq. 9. The large scatter observed in quasi-isotropic laminate data for high values of crack density is mainly due to the superposition of other damage modes (i.e. delamination) that can influence the laminate behavior. Results from the two laminates are superimposed in fig. 10 and show good agreement, thus indicating that the R-curve approach is suitable for predicting matrix crack growth in 90° plies of a laminate, when the cracked 90° plies are surrounded by 0° plies of the same material.

5. FREE EDGE DELAMINATION

A model for stiffness loss and strain energy release rate for free edge delamination onset and growth in graphite/epoxy laminates has been presented by O'Brien [2]. In this model, stiffness decreases linearly as delamination size increases and can be expressed by

$$E_x = E_0 - (E_0 - E^*)\frac{a}{b} \qquad (10)$$

where E_0 is the laminate modulus before delamination, a/b is the ratio of delamination size to specimen width, and E^* is the modulus of the laminate completely delaminated along one or more interfaces.

The delaminated modulus, E^*, can be calculated as the sum of the products of the moduli and thicknesses of the sublaminates which are created by the delamination. That is

$$E^* = \frac{\sum_{i=1}^{M} E_i t_i}{t} \qquad (11)$$

where t_i and E_i are the thickness and the moduli of the i^{th} sublaminate and M is the total number of sublaminates. The strain energy release rate for edge delamination can be evaluated by differentiating eq. 10 with respect to a and substituting into eq. 4 as shown in ref. 2,

$$G = \frac{\varepsilon^2 t}{2}(E_0 - E^*) \qquad (12)$$

The critical value of strain energy release rate G_c for edge delamination is obtained from the actual onset strain ε_c. This approach has been demonstrated to be useful for evaluating and predicting free edge delamination onset and growth in graphite/epoxy laminates [14].

For glass/epoxy laminates, the same approach has been attempted. However, several differences were noted. In graphite/epoxy, stiffness loss due to 90° ply matrix cracking was small [2,6], while this is not the case for glass/epoxy laminates [9-11,13]. In addition, because G for 90° ply matrix cracking is higher for glass/epoxy than graphite/epoxy laminates with the same layup (fig.8), and because the glass/epoxy has a lower Poisson mismatch, included in the $(E_0 - E^*)$ term of eq. 12, and hence a lower driving force for edge delamination than graphite epoxy, the glass/epoxy laminate is more likley to have extensive matrix cracking before the onset of delamination. These matrix cracks influence the stress and strain field in the region where the delamination will grow and they act as a delamination resistance mechanism [18-20]. Also, in glass/epoxy, because of the lower Poisson ratio mismatch, edge delaminations grow only a little in quasi-static conditions before the final 0° fiber failure. Furthermore, for the glass-epoxy laminates tested in fatigue, the effect of delamination on laminate stiffness loss is partially obscured by the simultaneous growth of ±45° matrix cracking, which was also observed previously for graphite epoxy [20].

As shown earlier in fig. 3, there are many contributions to stiffness loss in a $[\pm 45/0/90]_s$ glass/epoxy specimen during a fatigue test. To evaluate the contribution of each damage mode, a multiple linear regression analysis was performed on stiffness loss data. Because the relationship between stiffness loss and edge delamination size is linear (eq.10), and because a linear approximation between stiffness loss and 90° ply matrix crack density seems reasonable (fig.5), a linear relationship was assumed between stiffness loss and angle ply matrix crack density, and 0/90 edge, and +45/-45 local interface delamination sizes, as follows:

$$\frac{E}{E_o} = a_o - a_1 D_{90} - a_2 D_{45} - a_3 D_{-45} - a_4 \left(\frac{a}{b}\right)_{\pm 45} - a_5 \left(\frac{a}{b}\right)_{0/90} \qquad (13)$$

The set of coefficients from a_0 to a_5, for which equation (13) best approximated the experimental data, was evaluated statistically. The result of this analysis is shown in Table 1A.

Tab.1 A. Multiple regression parameters from FATIGUE TESTS

damage type	parameter	regression	std. dev.
undamaged condition	a_0	.9945	.0042
90° ply matrix cracking	a_1	.0674	.0048
+45° ply matrix cracking	a_2	.0415	.0175
-45° ply matrix cracking	a_3	.0238	.0076
+45/-45 interface delamination	a_4	.3211	.0302
0/90 interface delamination	a_5	.1488	.0357

Coefficient of determination = 0.89

Tab.1 B. Multiple regression parameters from STATIC TESTS

damage type	parameter	regression	std.dev
undamaged condition	a_0	1.00	.004
90° ply matrix cracking	a_1	.11	.005
0/90 interface delamination	a_5	.10	.039

Coefficient of determination = 0.92

As previously shown in fig.3, the 0/90 interface edge delamination and the angle ply cracking occur simultaneously. Therefore, the a_2, a_3, and a_5 coefficients are given by the regression analysis with a high degree of uncertainty. The contribution of each damage mode to stiffness loss is represented by the product of the regression coefficient in Table 1A and the appropriate damage parameter in eq. 13. Therefore, the regression parameters alone do not indicate the relative contribution of each damage mode to stiffness loss. For example, the analysis indicated an a_2 value that was nearly twice a_3, but fig.3(a) shows that the crack density in the -45° plies is nearly three times the density in the +45° plies. Hence, the external 45° matrix cracks had less influence on the laminate stiffness loss than the internal -45° matrix cracks. Unfortunately, there is currently no analytical model that directly relates stiffness loss to angle ply matrix crack density to verify this observation.

In order to achieve a better experimental evaluation of the edge delamination contribution to stiffness loss in the quasi-isotropic laminate, a similar statistical analysis was applied to the static test data, where only 90° ply cracks and edge delaminations were found. For this special case, eq.13 reduces to:

$$\frac{E}{E_0} = a_0 - a_1 D_{90} - a_5\left(\frac{a}{b}\right) \qquad (14)$$

The set of coefficients obtained for this three parameter regression analysis is reported in Table 1B. Dividing eq.10 by E_0 and comparing to eq.14 indicates that $a_0 = 1$, and that

$$a_5 = (E_0 - E^*)/E_0 \qquad (15)$$

Therefore, a direct comparison may be made between a_5 calculated from the regression analysis and the value calculated from laminated plate theory using eq.15. According to the regression analysis, the delamination contribution to the longitudinal modulus loss gives an (E_0-E^*) value of 2500 MPa. However, using laminated plate theory to evaluate the terms in eq.15 yields an (E_0-E^*) value ranging from 1020 MPa to 770 MPa, depending whether or not the preexisting 90° ply matrix cracks are considered. Hence, G determined using (E_0-E^*) from experiments, where significant 90° ply matrix cracks exist ahead of the delamination front, would be larger than G determined from calculated properties. This observation is consistent with previous studies that showed an edge delamination resistance curve could be generated and correlated with the increase in 90° ply matrix crack density [2,19,20].

These results suggest that the interlaminar stress field near the delamination front in the 0/90 interface is influenced by the presence of 90° ply matrix cracking. A three dimensional model is required to accurately account for the interaction between matrix cracks and delamination.

6. FRACTURE TOUGHNESS EVALUATION

From the analysis above, critical strain energy release rate values were obtained for both matrix cracking, eq.(9), and edge delamination, eq.(12), in static tension and tension-tension fatigue, and are shown in Table 2. In both cases dE/dA values, used to calculate strain energy release rate, were taken from experimental results. The G_c for matrix cracking and edge delamination both decreased dramatically in fatigue compared to the static values. This is consistent with similar data generated on graphite reinforced composites with a variety of matrices [21-23]. The G_c for delamination was found to be higher than the G_c for matrix cracking. Although different fracture modes are involved for these two mechanisms, this mode difference is not sufficient to explain the

large observed difference in G_c. Other sources [15] report a static G_{Ic} for matrix cracking of reinforced epoxy composites similar to the measured value reported in Table 2. The problem of evaluating G_c for delamination onset is again closely connected to the evaluation of the stiffness loss due to delamination and is, therefore, affected by the uncertainties reported in the previous section. However a comparison with data previously obtained on different composites materials [16] showed that the values reported in Table 2 for static and fatigue onset were at least congruent with those data.

damage	load condition	Gc
90° ply matrix cracking	static tension	120 J/m²
90° ply matrix cracking	tension-tension fatigue	30 J/m²
0/90 interface delamination	static tension	460 J/m²
0/90 interface delamination	tension-tension fatigue	110 J/m²

TABLE II. Measured critical strain energy release rate for T190/x751/50.

7. CONCLUDING REMARKS

The purpose of this work was to study damage onset, accumulation and its consequences on glass/epoxy multidirectional laminates using simple stress analysis tools and fracture mechanics. The relatively lower stiffness of glass fibers compared to graphite fibers and the higher strains involved in damage and failure processes have highlighted the considerable importance of matrix cracks parallel to the fibers. Glass-fiber laminates are useful in studying matrix cracking but they show incongruences when other failure modes, such as edge delamination, are superimposed.

A simple way to model stiffness reduction due to cracked 90° ply matrix was verified and shown to apply over a wide range of crack densities using both F.E.M. analysis and experiment.

A closed form expression for strain energy release rate associated with matrix cracking has been proposed and, following experiments, strain energy release rate resistance curves (R-curves) for two different layups of the same material have been shown to coincide fairly well. The strain energy release rate approach used in this study can help explain the observed saturation crack density for matrix cracking.

Edge delamination was difficult to analyze using the conventional tools developed for graphite reinforced composites. The superposition of matrix cracking leads to an overestimation of the interlaminar fracture toughness. Further investigation in this field is needed.

8. REFERENCES

1. S.Tsai, H.T.Hahn — Introduction to Composite Materials, Technomic Publ.Co., Stamford CT, 1980
2. T.K.O'Brien — "Characterization of Delamination Onset and Growth in a Composite Laminate", in Damage in Composite Materials, ASTM STP 775, 1982, pp.140-167
3. J.M.Whitney, M.Knight — "A modified Free Edge Delamination Specimen", in Delamination and Debonding of Materials, ASTM STP 876, 1985, pp.298-314

4. T.K.O'Brien, I.S.Raju and D.P.Garber — "Residual Thermal and Moisture Influences on the Strain Energy Release Analysis of Edge Delamination", ASTM Journal of Composites Technology and Research, Vol.8, No.2, Summer 1986.

5. A.S.D.Wang, F.W.Crossman — "Initiation and Growth of Transverse Cracks and Edge Delamination in Composite Laminates Part 1: an Energy Method", J. Composite Materials Supplement, Vol.14, 1980, pp.71-87.

6. J.T.Ryder ,F.W.Crossman — "A Study of Stiffness, Residual Strength and Fatigue Life Relationships for Composite Laminates", NASA Contract Report CR-172211, Oct 1983.

7. F.W.Crossman,A.S.D.Wang — "The Dependence of Transverse Cracking and Delamination on Ply Thickness in Graphite/Epoxy Laminates", in Damage in Composite Materials, ASTM STP 775, 1982, pp.118-139.

8. K.L.Reifsnider E.G.Henneke and W.W.Stinchcomb — "Defect-Property Relationships in Composite Materials" ,AFML-TR-76-81, Part IV, Air Force Materials Lab. , June 1979.

9. A. L. Highsmith and , K.L.Reifsnider — "Stiffness Reduction Mechanisms in Composite Laminates", ASTM STP 775, 1982, pp.103-117.

10. A.Parvizi, K.W.Garrett and J.E.Bailey, — "Constrained Cracking in Glass Fibre Reinforced Epoxy Cross-Ply Laminates", J. of Materials Science, Vol.13, 1978, pp.195-201.

11. M.G.Bader, J.E.Bailey, T.P.Curtis and A.Parvizi — "The Mechanisms of Initiation and Development of Damage in Multi-Axial Fibre Reinforced Plastic Laminates", Proc. 3rd Symp. on Mechanical Properties of Materials, Cambridge, U.K.,Aug 1979, Vol.3, pp.227-238.

12. D.L.Flaggs and M.H.Kural — "Experimental determination of the In Situ Transverse Lamina Strength in Graphite/Epoxy Laminates", J. Composite Materials, Vol.16, 1982, pp.103-116.

13. S.L.Ogin,P.A.Smith and P.W.R.Beaumont — "Matrix Cracking and Stiffness Reduction during the Fatigue of a $[0/90]_s$ GFRP Laminate", Composites Science and Technology, Vol.22, 1985, pp.23-31.

14. T.K.O'Brien,N.J.Johnston I.S.Raju,D.H.Morris and R.A.Simonds — "Comparisons of various Configurations of The Edge Delamination Test for Interlaminar Fracture Thoughness", in Toughened Composites, ASTM STP 937, 1987.

15. G.E.Law — "A Mixed-Mode Fracture Analysis of $[\pm 25/90_n]_s$ Graphite/Epoxy Composite Laminates", ASTM STP 836, 1984, pp.143-160.

16. T.K.O'Brien,N.J.Johnston D.H.Morris and R.A.Simonds — "A Simple Test for the Interlaminar Fracture Toughness of Composites", SAMPE Journal, Vol.18, No.4, July 1982, pp.8-15.

17. G.R.Irwin — "Fracture," Handbuch der Physik, vol.6, 1958, p.551

18. A.Poursartip — "The Characterization of Delamination and Matrix Crack Growth in Laminates under Fatigue Loading", in Toughened Composites, ASTM STP 937, 1987.

19.	T.K.O'Brien	"Interlaminar fracture of Composites",Journal of Aero. Soc. of India, vol.37, 1985, p.61.
20.	T.K.O'Brien	"Tension Fatigue behavior of Quasi-isotropic Graphite/Epoxy laminate", Proc.3rd Risoe International Symposium on Metallurgy and Material Science, 6-10 sept. 1982.
21.	T.K.O'Brien	"Mixed-mode Strain Energy Release Rate Effects on Edge Delamination of Composites",in Effects of Defects in Composite Materials, ASTM STP 836, 1984
22.	D.F.Adams,R.S.Zimmerman and E.M.Odem	"Determining Frequency and Load Ratio Effect on the Edge Delamination Test in Graphite/Epoxy Composites", in Toughened Composites, ASTM STP 937, 1987.
23.	T.K.O'Brien	"Fatigue Delamination Behavior of PEEK Thermoplastic Composite Laminates", Proceedings of the American Society for Composites First Conference on Composite Materials, Dayton, Ohio, October 7-9, 1986.
24.	M.Caslini,C.Zanotti, and T.K.O'Brien	"Fracture Mechanics of Matrix Cracking and Delamination in Glass/Epoxy Laminates.", NASA TM-89007, Aug.1986.

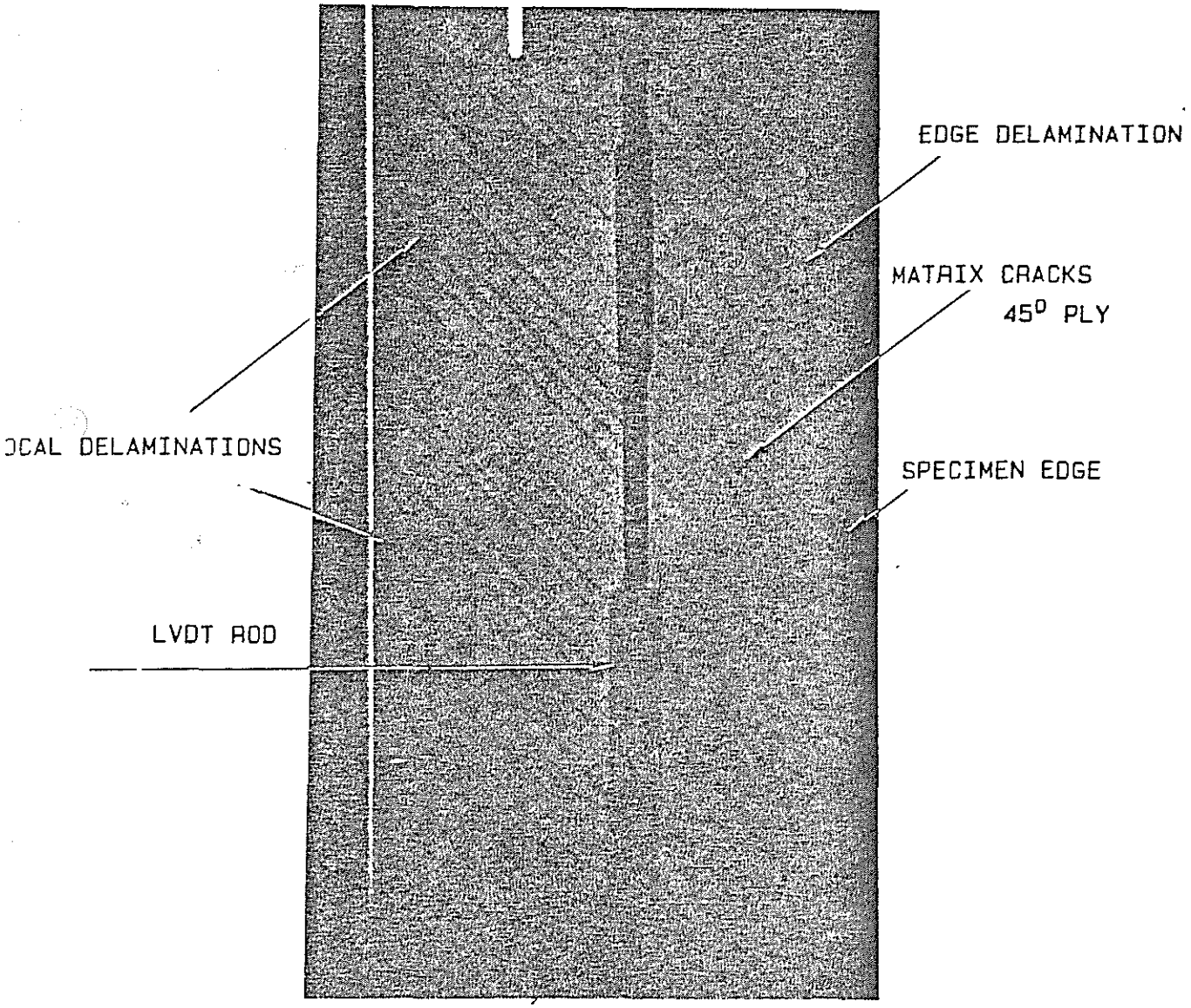

Fig.1 : Photograph of a quasi isotropic [±45/0/90] glass-epoxy specimen, during fatigue test.

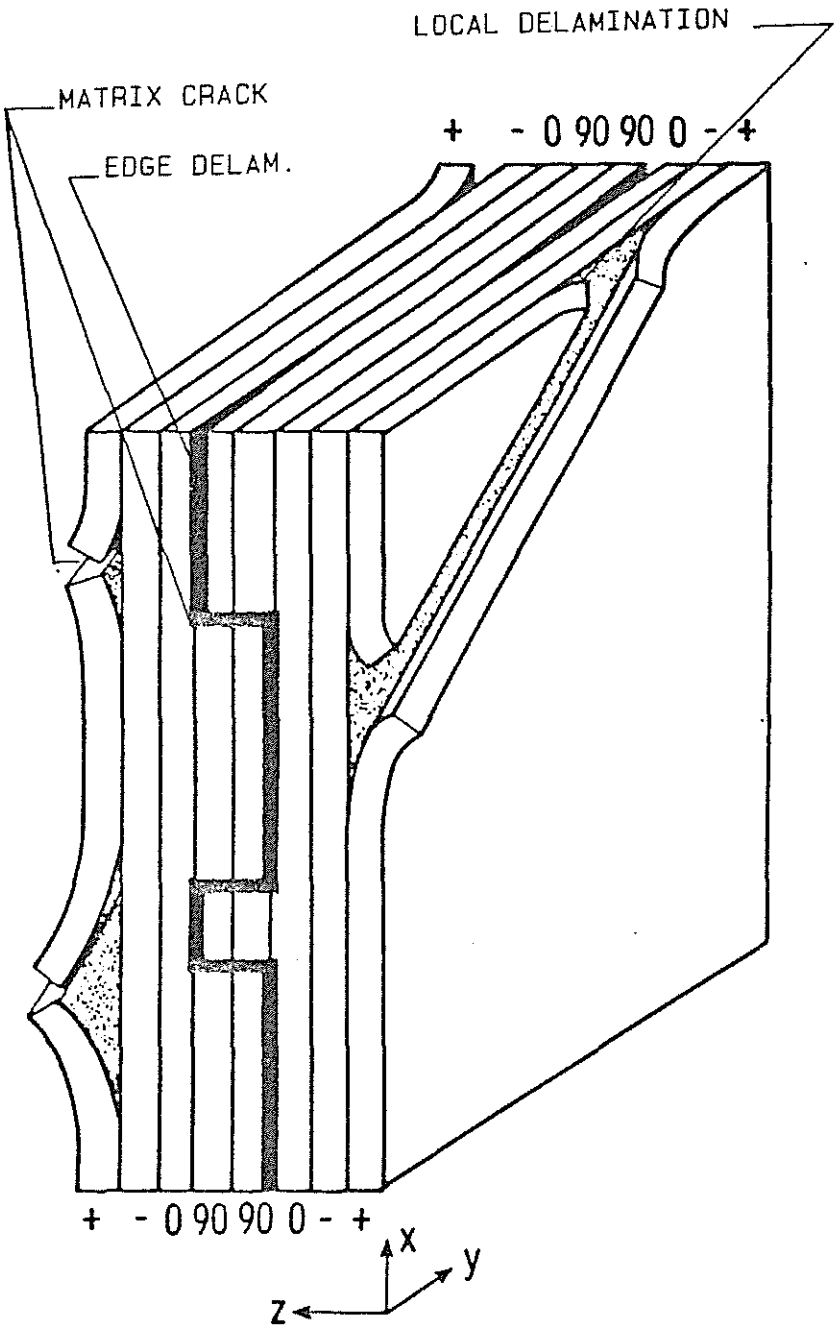

Fig.2 : Schematic picture of possible damage modes of quasi isotropic layup.

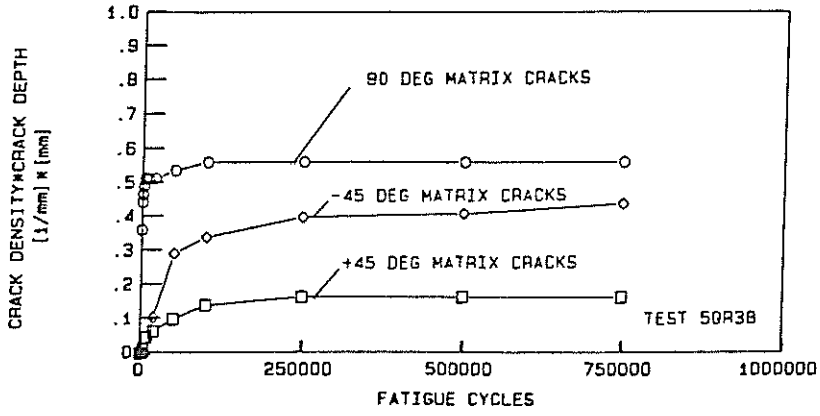

Fig.3(a)

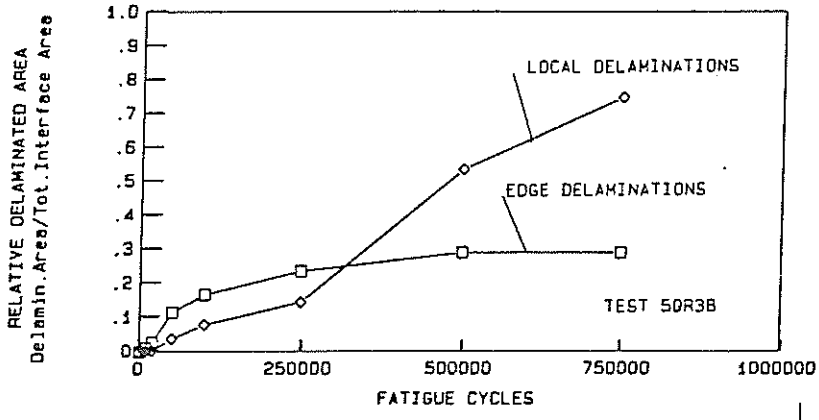

Fig.3(b)

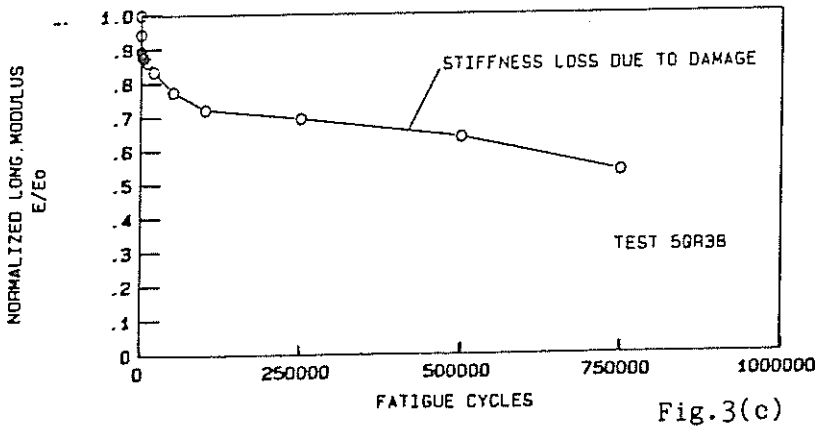

Fig.3(c)

Fig.3 : Damage accumulation in a typical fatigue test on a $[\pm 45/0/90]_s$ specimen. R=0.1, σ_{max}=160 MPa, Cycles to failure are 792300.

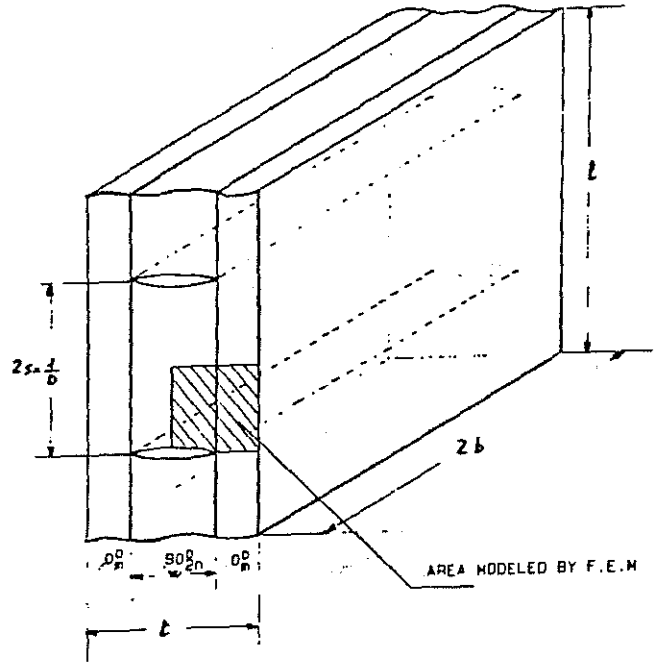

Fig.4 : Matrix cracking in a $[0/90]_s$ laminate.

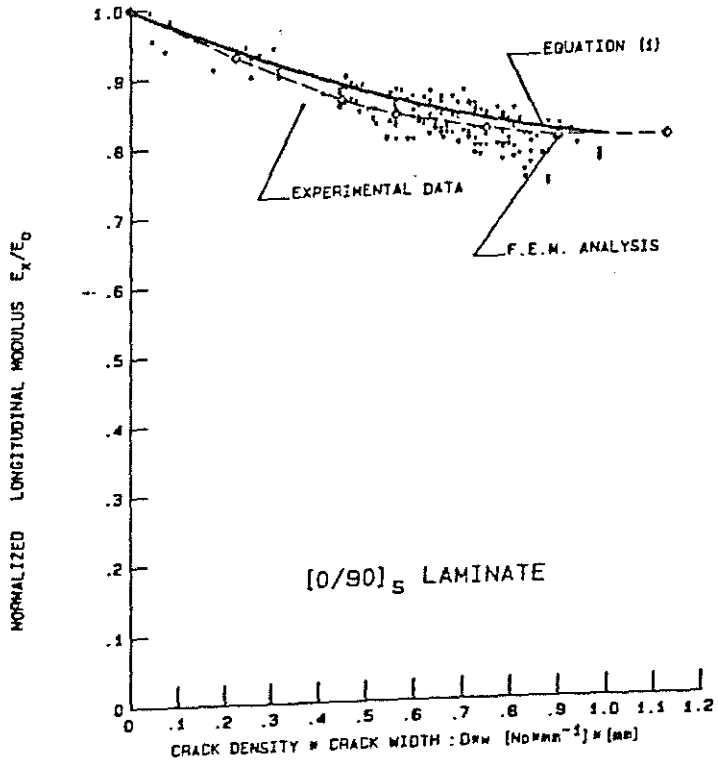

Fig.5 : Stiffness loss in static and fatigue tests on $[0_m/90_n]_s$ glass/epoxy laminate.

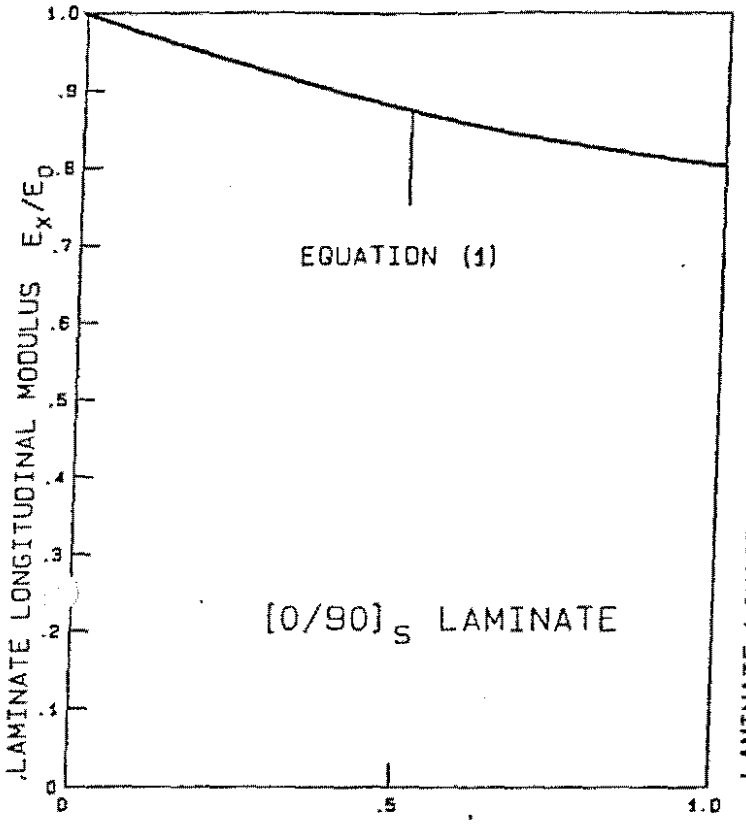

Fig.6(a)

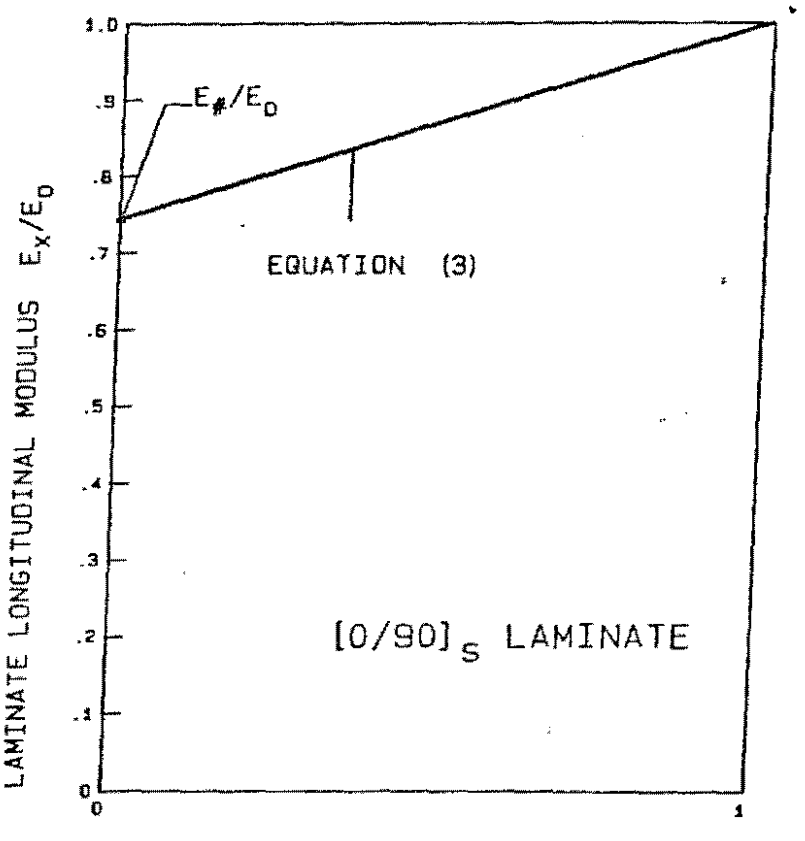

Fig.6(b)

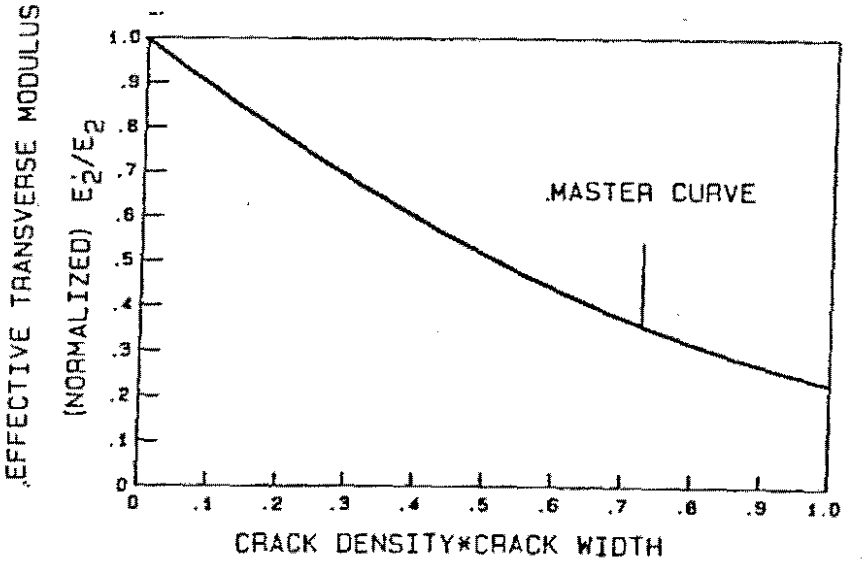

Fig.6(c)

Fig.6 : Evaluation of 90° ply matrix cracking effect on generic laminate stiffness.

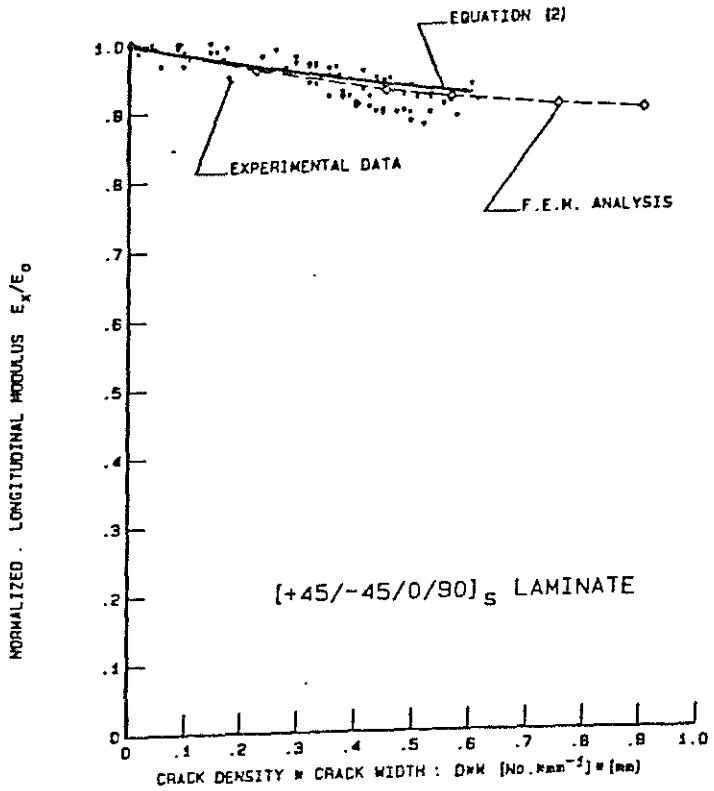

Fig.7 : Stiffness loss in the initial part of fatigue tests on $[\pm 45/0/90]_S$ glass/epoxy laminate due to 90° ply matrix cracking.

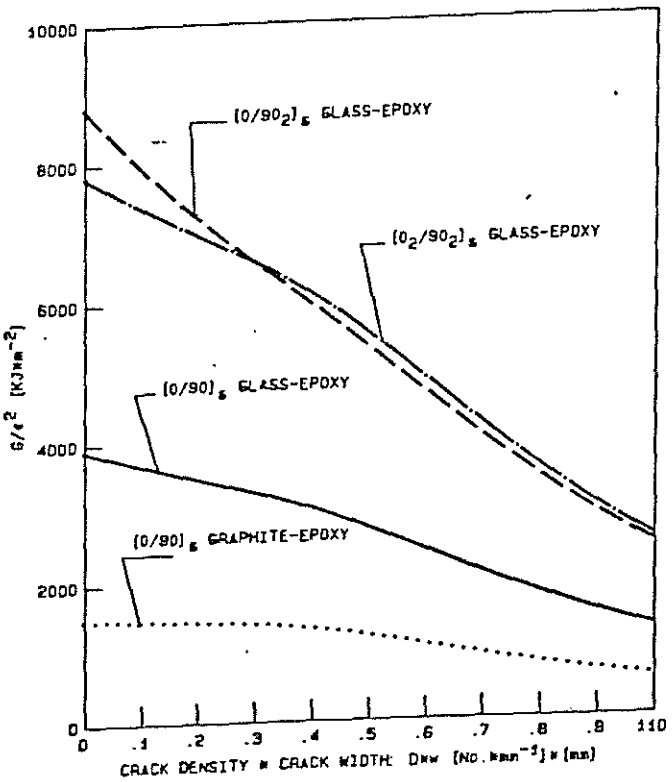

Fig.8 : Strain Energy Release Rate versus matrix crack density for different laminates.

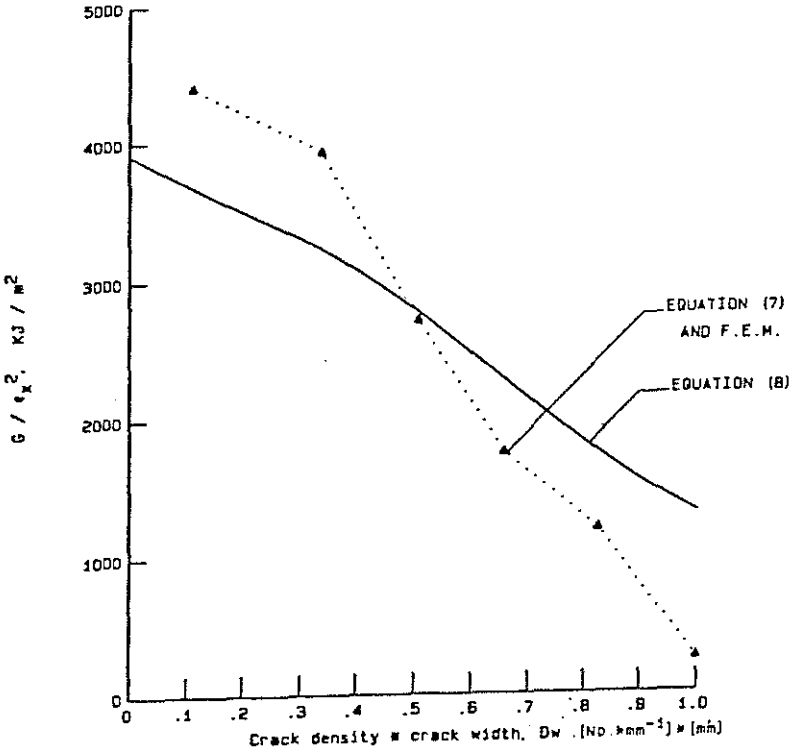

Fig.9 : Comparison of Strain Energy Release Rate from analytical model (eq.8) and finite element analysis in a $[0/90]_s$ glass-epoxy laminate.

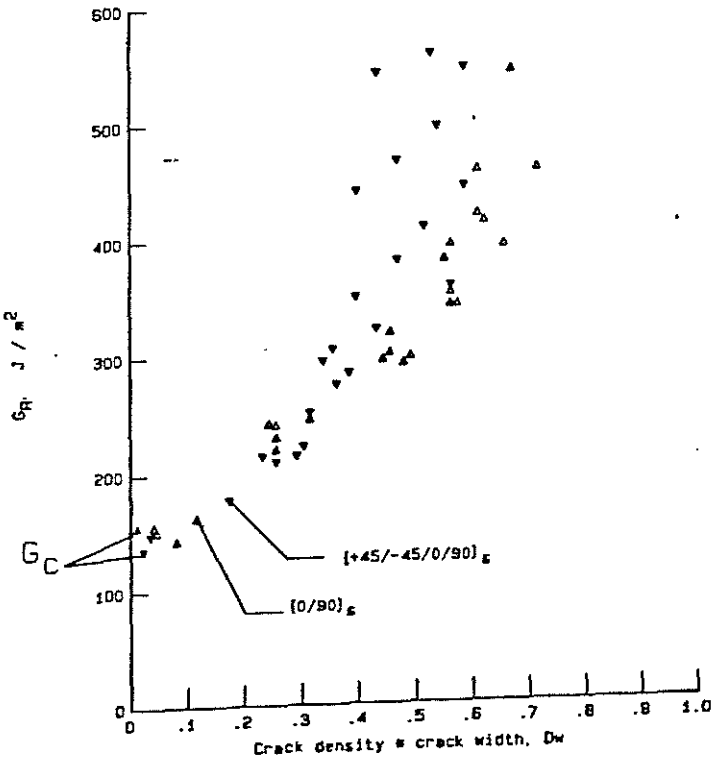

Fig.10: Matrix cracking resistance curves for 90° ply matrix cracking in $[0/90]_s$ and $[\pm 45/0/90]_s$ glass epoxy laminate.